J Huazhong Univ Sci Technol［Med Sci］
DOI 10.1007/s11596-012-0051-5 32(2):291-298,2012

Inhibition of Glial Activation in Rostral Ventromedial Medulla Attenuates Mechanical Allodynia in a Rat Model of Cancer-induced Bone Pain*

Xijiang LIU (刘希江), Huilian BU (卜慧莲), Cheng LIU (刘 成), Feng GAO (高 峰), Hui YANG (杨 辉), Xuebi TIAN (田学愎), Aijun XU (许爱军), Zhijun CHEN (陈治军), Fei CAO (曹 菲)#, Yuke TIAN (田玉科)#
Department of Anesthesiology, Tongji Hospital, Tongji Medical College, Huazhong University of Science and Technology, Wuhan 430030, China

Summary: Descending nociceptive modulation from the supraspinal structures plays an important role in cancer-induced bone pain (CIBP). Rostral ventromedial medulla (RVM) is a critical component of descending nociceptive facilitation circuitry, but so far the mechanisms are poorly known. In this study, we investigated the role of RVM glial activation in the descending nociceptive facilitation circuitry in a CIBP rat model. CIBP rats showed significant activation of microglia and astrocytes, and also up-regulation of phosphorylated p38 mitogen-activated protein kinase (p38 MAPK) and pro-inflammatory mediators released by glial cells (IL-1β, IL-6, TNF-α and brain-derived neurotrophic factor) in the RVM. Stereotaxic microinjection of the glial inhibitors (minocycline and fluorocitrate) into CIBP rats' RVM could reverse the glial activation and significantly attenuate mechanical allodynia in a time-dependent manner. RVM microinjection of p38 MAPK inhibitor (SB203580) abolished the activation of microglia, reversed the associated up-regulation of pro-inflammatory mediators and significantly attenuated mechanical allodynia. Taken together, these results suggest that RVM glial activation is involved in the pathogenesis of CIBP. RVM microglial p38 MAPK signaling pathway is activated and leads to the release of downstream pro-inflammatory mediators, which contribute to the descending facilitation of CIBP.
Key words: cancer-induced bone pain; microglia; astrocyte; p38 MAPK; rostral ventromedial medulla

Cancer-induced bone pain (CIBP) is a very common clinical problem in the cancer patients, especially with those in the terminal phase. It seriously affects the life quality and significantly shortens the lifetime of patients. Unfortunately, so far, its mechanisms remain poorly understood and clinically very few effective treatments without obvious adverse effects are available[1–3]. The mechanisms of CIBP involved, possibly, neuropathic, inflammatory and tumorous factors. For example, various pro-hyperalgesic mediators released by local infiltrating tumor cells, inflammatory cells, osteoclasts and osteoblasts induce sensitization of peripheral and central nervous systems and all contribute to the development of CIBP[4]. Accumulating evidence demonstrated that, during pathological pain status, sensitized peripheral sensory nerves continuously transmit nociceptive signals to the supra-spinal areas, thereby changing the neural plasticity of supra-spinal areas, including activation of descending nociceptive facilitatory system from rostral ventromedial medulla (RVM)[5–7]. Then, sensitized neurons in the RVM could project neurotransmitters (e.g., monoamines) to the spinal cord to maintain spinal sensitization. Moreover, descending facilitation induces the release of pro-nociceptive excitatory neurotransmitters from primary afferent terminals (glutamate, substance P, neuropeptide Y, *etc*.), and is an imperative factor for maintaining pathological pain[5, 8]. Therefore, blocking descending nociceptive facilitation arising from RVM could alleviate pathological pain[9].

It was recently reported that activated RVM glial cells also played an important role in the development of inflammatory and neuropathic pain. Both plantar subcutaneous injection of carrageenan[10] and chronic constriction injury of the rat infra-orbital nerve[11] could result in activation of RVM glia. In activated microglia, pro-inflammatory cytokine promoter p38 mitogen-activated protein kinase (p38 MAPK) became phosphorylated, and then facilitated the release of pro-inflammatory substances, such as cytokines (e.g. IL-1β, IL-6, TNF-α), nerve growth factor [e.g. brain-derived neurotrophic factor (BDNF)], excitatory amino acids, and so on[12]. These substances further sensitized neurons and glial cells and enhanced descending nociceptive facilitation. Therefore, either inhibiting activation of RVM glia or eliminating produc-

Xijiang LIU, E-mail: xijiang_liu@163.com
#Corresponding author, Fei CAO, E-mail: doctor.caofei@hotmail.com; Yuke TIAN, E-mail: yktian@tjh.tjmu.edu.cn
*This project was supported by grants from the National Natural Science Foundation of China (No. 30901396, No. 81070890, No. 30872441 and No. 81171259).

tion of focal pronociceptive substances from activated glial cells may effectively abolish pain[13].

CIBP is a unique pain state, which differs from inflammatory and neuropathic pain. To our knowledge, most of previous studies investigating glial roles in CIBP focused more on alternations within the spinal cord[14, 15]. In this study, our attention was directed at the roles of glia in the RVM and the relationship between RVM glia and descending nociceptive facilitation in CIBP.

1 MATERIALS AND METHODS

1.1 Animal Grouping and Treatment

All animal procedures were carried out in accordance with the NIH guidelines and Ethical Issue of the IASP and were approved by the Experimental Animal Care and Use Committee of Tongji Medical College, Huazhong University of Science and Technology (HUST) Wuhan, China. Female Sprague-Dawley rats, weighing 160–180 g, supplied by the Experimental Animal Center, Tongji Medical College, HUST, were housed in a temperature-controlled room (22–24°C) with free access to food and water on a 12-h light/dark cycle. The rats were randomly divided into eight groups: (1) Naive group (n=6), in which no intervention was given; (2) Sham group (n=18), in which 10-μL D-hank's solution was injected into the right tibia; (3) CIBP group (n=18), in which 10-μL Walker 256 breast cancer cell suspension (3×10^4) was injected into the right tibia; (4) Sham/NS group (n=15), in which 0.5-μL normal saline was injected into RVM 10 days after sham operation; (5) CIBP/NS group (n=15), in which 0.5-μL normal saline was injected into RVM 10 days after CIBP modeling; (6) CIBP/minocycline group (n=12), in which 0.5-μL (25 μg) microglial inhibitor minocycline was injected into RVM 10 days after CIBP modeling; (7) CIBP/fluorocitrate group (n=12), in which 0.5-μL (1 μg) astrocyte inhibitor fluorocitrate was injected into RVM 10 days after CIBP modeling; (8) CIBP/SB203580 group (n=15), in which 0.5-μL (10 μg) p38MAPK inhibitor SB203580 was injected into RVM 10 days after CIBP modeling.

1.2 CIBP Modeling

The CIBP model was induced as previously reported[16]. Briefly, rats were anesthetized with chloral hydrate (300 mg/kg, i.p.). The right leg was shaved and disinfected. About 1-cm rostral-caudal incision was made in the skin over the top medial half of the tibia. By using a 23-gauge needle, the bone was pierced approximately 0.5–1 cm below the knee joint distal to the epiphysial growth plate. Then, the needle was removed and replaced with a 50 μL Hamilton microsyringe containing Walker 256 carcinoma cells or D-hank's solution. A volume of 10 μL carcinoma cells (3×10^4) was slowly injected into the bone cavity. The injection site was closed with bone wax.

1.3 Radiological Examination of Bone

Tibial destruction was radiographically examined (Kodak Directview DR3000 system, Eastman Kodak Co., USA). Rats were exposed to an X-ray source under chloral hydrate (300 mg/kg, i.p.) anesthesia on day 10, 15 and 20 after cancer cell inoculation.

1.4 RVM Drug Microinjection

Rats were anesthetized by using propofol (50 mg/kg, i.p.)[17], and placed in a stereotaxic instrument. A midline incision was made after infiltration of lidocaine (2%) into the skin. A midline opening was made in the skull to insert a microinjection needle into the target site. The coordinates for RVM were as follows: –10.5 mm caudal to bregma, midline, and –9.0 mm ventral to the surface of the cerebellum (Paxinos and Watson, 2005). Microinjection was performed by delivering 0.5-μL drug solution slowly over a 30-s period by using a 0.5-μL Hamilton syringe with a 32 gauge needle. The injection needle was left in place for at least 5 minutes before withdrawal [18]. The followings inhibitors were used: minocycline hydrochloride (#M9511, Sigma, USA) was freshly dissolved daily in distilled H_2O; fluorocitrate (#F9634, Sigma, USA) was first dissolved in 1 N HCl and then diluted in 0.9% sterile, isotonic saline; the p38 MAPK inhibitor SB203580 hydrochloride (#S8307, Sigma, USA) was dissolved in distilled H_2O; normal saline was microinjected into RVM, serving as the control.

1.5 Behavioral Assessment

Mechanical allodynia was assessed by measuring hind paw withdrawal thresholds (PWT) to von Frey filament stimulation, applied to the plantar surface in ascending order of force (0.16–15.0 g) for up to 6 s per filament. Once a withdrawal response was established, the paw was re-tested, starting with the next descending von Frey hair until no response occurred. The lowest amount of force required to elicit a positive response was recorded as the PWT, represented in gram (g)[19, 20].

1.6 Immuno-based Analysis

Immunohistochemistry and glial response state scoring were performed as described previously[21]. Briefly, scoring was on a 4-point scale as follows: 0: unactivated; +: mild activation; ++: moderate activation; +++: intense activation. For Western blotting, identical amounts (50 μg) of total proteins from the RVM were separated on 10% SDS-PAGE gels, and then trans-blotted to PVDF membranes. The following primary antibodies were used: antibodies against glial fibrillary acidic protein (GFAP, 1:400, Millipore, USA), ionized calcium-binding adaptor molecule 1 (Iba1, 1:500, Santa Cruz, USA), phospho-p38 MAPK (p-p38 MAPK, 1:400, Cell Signaling Technology, USA) and β-actin (1:1000, Santa Cruz). For densitometric analysis, blots were scanned and quantified with GeneSnap v6.05 software package (England) and the results were expressed as a ratio of target to β-actin immunoreactivity[22].

1.7 Real-time Polymerase Chain Reaction (PCR)

Under chloral hydrate (300 mg/kg, i.p.) anesthesia, on the 4th, 7th, 10th, 15th and 20th postoperative day, RVM tissues from sham and CIBP groups were quickly removed, and snap-frozen in liquid nitrogen for analysis of mRNA of ITGAM and GFAP. On the 10th postoperative day, 30 min after RVM injection of SB203580, RVM tissues from sham/NS, CIBP/NS and CIBP/SB203580 groups were also collected for analysis of mRNA of IL-1β, IL-6, TNF-α and BDNF. All samples (n=3 per time-point) were stored at −80°C until assay. Primer sequences for the genes of interest were designed and synthesized by Invitrogen, USA (table 1). RNA ex-

traction, cDNA synthesis and real-time PCR were performed as reported previously[16]. The levels of target mRNA were quantified relative to levels of the housekeeping gene GAPDH by using the relative quantification $2^{-\Delta\Delta CT}$ method.

Table 1 Primers for the real-time PCR

Target genes	GenBank accession no.	Primers	Product length (bp)
GAPDH	NM_017008.3	Forward: 5'-GGCACAGTCAAGGCTGAGAATG-3'	143
		Reverse: 5'-ATGGTGGTGAAGACGCCAGTA-3'	
ITGAM	NM_012711.1	Forward: 5'-CTGCCTCAGGGATCCGTAAAG-3'	150
		Reverse: 5'-CCTCTGCCTCAGGAATGACATC-3'	
GFAP	NM_017009	Forward: 5'-TGGCCACCAGTAACATGCAA-3'	134
		Reverse: 5'-CAGTTGGCGGCGATAGTCAT-3'	
IL-1β	NM_031512.2	Forward: 5'-GTGGGATGATGACGACC -3'	151
		Reverse: 5'-CACTTGTTGGCTTATGTTCT -3'	
IL-6	NM_012589.1	Forward: 5'-TCAACTCCATCTGCCCTTCAG-3'	70
		Reverse: 5'-AAGGCAACTGGCTGGAAGTCT-3'	
TNF-α	NM_012675.3	Forward: 5'-AACTGGCAGAGGAGGCG -3'	115
		Reverse: 5'-CAGAAGAGCGTGGTGGC -3'	
BDNF	NM_012513.3	Forward: 5'-GAGCTGAGCGTGTGTGACAG-3'	278
		Reverse: 5'-CGCCAGCCAATTCTCTTTTTGC-3'	

1.8 Data Analysis

Raw data were presented as $\bar{x}\pm s_{\bar{x}}$ and changes in means within each group over time were analyzed by using one-way ANOVA, followed by *post hoc* comparison (Student-New-man–Keuls test). Significant differences between treatment groups were detected by two-way ANOVA. A $P<0.05$ was considered to be statistically significant.

2 RESULTS

2.1 Radiological Detection of Tibia Destruction

Tibia destruction by tumor was radiographically dectected. No structural destruction was observed in sham group (fig. 1A). In contrast, in CIBP rats the radiographs showed mild bone destruction on day 10 (fig. 1B). The bone destruction exhibited progressive worsening on day 15 (fig. 1C) and 20 (fig. 1D).

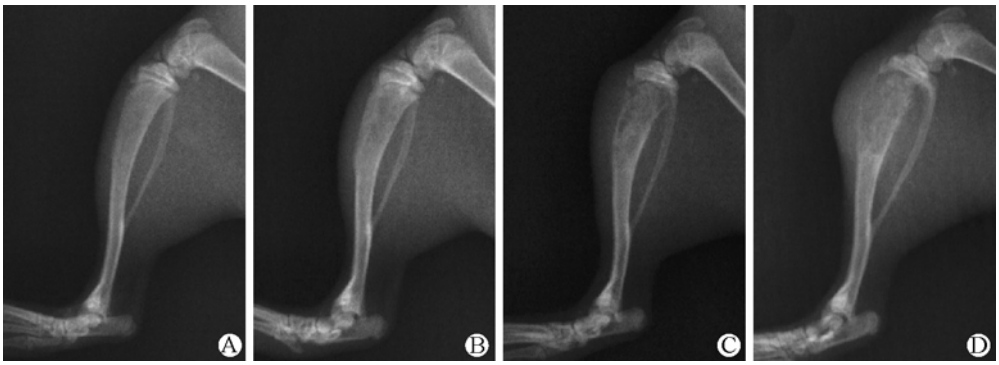

Fig. 1 Tibial radiographs of tested rats

Radiographs of ipsilateral tibia from sham-operated rats on day 20 after inoculation showed intact bone (A), while tibia from CIBP group on day 10 after inoculation showed mild bone destruction (B), on day 15 (C) and 20 (D) after inoculation exhibited evident bone destruction.

2.2 Glial Aactivation in the RVM of CIBP Rats

Compared with naive and sham groups, the mRNA expression of ITGAM (microglial marker) and GFAP (astrocytic marker) was significantly increased in CIBP rats ($P<0.05$) from the 10th day after walker 256 rat mammary gland carcinoma cells inoculation (table 2). Therefore, this time point was chosen for further study. Rats were sacrificed 10 days after intra-tibia inoculation of carcinoma cells or D-hank's solution, and then brainstem tissues were prepared for immunodetection of OX-42 (microglia) or GFAP (astrocyte) (n=3 per group). The scores of glial response states of RVM sections were: '0' (fig. 2A and 2C) and '+++' (fig. 2B and 2D), respectively, suggesting that both microglia and astrocytes were activated in CIBP rats. Activated microglia and astrocytes exhibited hyper-trophied cell bodies and increased cell numbers (fig. 2B and 2D) as compared with corresponding cells from sham-operated rats (fig. 2A and 2C).

2.3 Reversing Effect of Microglial Inhibitor on Pain Hypersensitivity in CIBP Rats

To investigate the effects of activated microglia on behavioral abnormalities in CIBP rats, the selective microglial inhibitor minocycline (25 μg) was microinjected into RVM[10, 23]. CIBP rats showed mechanical allodynia on the 10th day, as indicated by significant reduction in paw withdrawal threshold (PWT) to 1.3±0.3 g from a baseline mean of 14.2±0.3 g (n=18, $P<0.05$) (fig. 3A).

Sham-operated rats showed no significant difference from the baseline (data not shown). Minocycline reversed mechanical allodynia in a time-related manner, with the peak analgesia effect being observed 30 min after injection and indicated by a mean PWT of 9.7 ± 0.3 g (n=6, P<0.05). PWTs returned to pre-microinjection levels 90 min after minocycline administration, as indicated by a mean PWT of 1.3±0.2 g (fig. 3A). Furthermore, in order to determine whether the inhibition of mechanical allodynia of CIBP rats by minocycline was related to inhibition of RVM microglial activation, the sections were obtained from sham-operated rats and CIBP rats between 15 and 45 min after RVM microinjection of minocycline or saline, then prepared for immuno-staining of the microglial marker OX-42. CIBP rats receiving saline injection showed increased OX-42 immuno-labeling (microglial response score: +++) (fig. 3D) relative to the sections from sham-operated group (microglial response score: 0) (fig. 3C). Importantly, RVM sections from CIBP rats receiving minocycline microinjection showed decreased immunofluorescent labeling for OX-42 (microglial response score: +) (fig. 3E) as compared with those from CIBP rats treated with vehicle (fig. 3D), indicative of reduced microglial activation. In CIBP rats, Iba1 (17 kD) showed significantly increased level 69.7%±4.0% (n=3, P<0.05) (fig. 3B) as compared with vehicle-treated sham-operated animals (28.7%±0.3%; n=3). RVM microinjection of minocycline resulted in reduced Iba1 protein level (24.7%±1.5%; n=3) and caused no significant difference (P>0.05) from that of saline-treated sham-operated animals (fig. 3B), indicating the profound inhibition of microglia activation. These results suggested that minocycline diminished RVM microglia activation in CIBP rats, and consequently reduced nociceptive hypersensitivity.

Table 2 The expression levels of ITGAM and GFAP mRNA in the RVM (n=3, $\bar{x}\pm s$)

Target genes	Naive	Sham					CIBP				
		Day after model establishment									
		4th	7th	10th	15th	20th	4th	7th	10th	15th	20th
ITGAM	0.96±0.07	0.92±0.06	1.02±0.04	1.08±0.09	1.05±0.06	1.00±0.09	0.99±0.07	1.27±0.23	2.02±0.10$^{*\#}$	3.49±0.18$^{*\#}$	1.46±0.08$^{*\#}$
GFAP	0.97±0.10	1.09±0.05	1.04±0.05	1.02±0.04	1.00±0.04	1.04±0.03	0.94±0.12	1.15±0.06	1.82±0.14$^{*\#}$	4.12±0.06$^{*\#}$	4.74±0.19$^{*\#}$

$^{*}P$ < 0.05, *vs.* naïve group; $^{\#}P$< 0.05, *vs*. sham-operated group

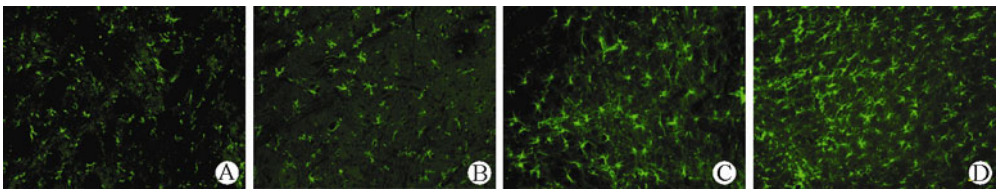

Fig. 2 Activation of microglia and astrocytes in RVM of CIBP rats

RVM sections were from sham-operated rats (A and C) or CIBP rats (B and D) and immuno-labeled by OX-42 (microglia; A and B) and GFAP (astrocytes; C and D). CIBP rats showed an increased labeling for OX-42 (B) and GFAP (D) along with morphological changes indicative of activation of glia (scale bar: 20 μm).

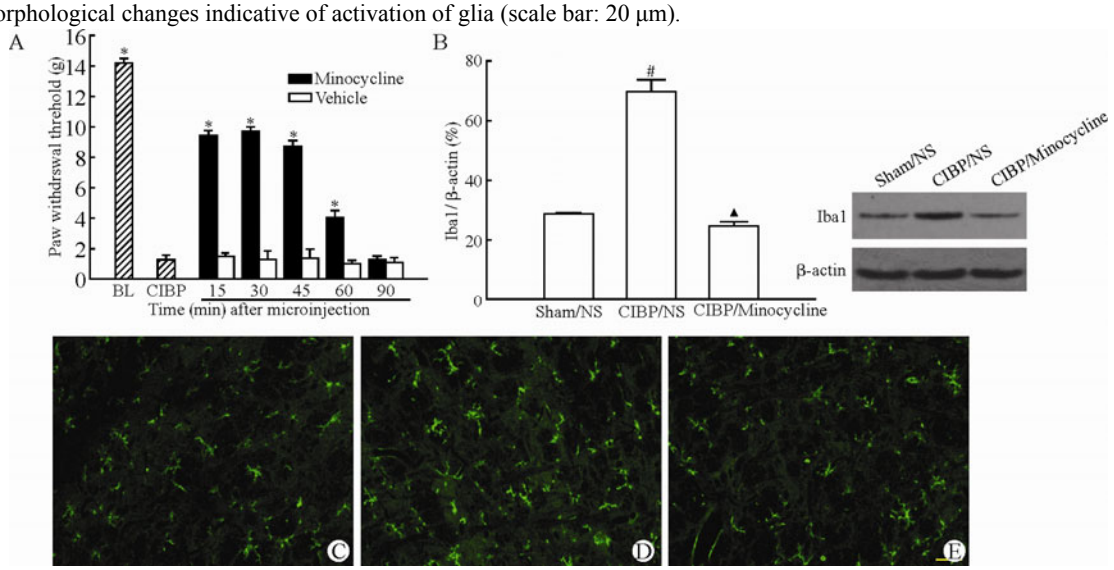

Fig. 3 Microglial inhibitor attenuated CIBP and reversed microglial activation.

A: RVM injection of minocycline attenuated mechanical allodynia time-dependently ($^{*}P$<0.05, *vs.* CIBP). B: RVM injection of minocycline reversed the up-regulation of Iba1 in CIBP rats ($^{\#}P$<0.05, *vs.* Sham/NS; $^{\blacktriangle}P$<0.05, *vs.* CIBP/NS). C: RVM sections from sham-operated rats receiving saline. D: RVM sections from CIBP rats given saline. E: RVM sections from CIBP rats administered minocycline at 25 μg. In CIBP rats, RVM injection of minocycline produced a reduction in immunofluorescence intensity for OX-42 along with morphological changes, suggesting reduced microglial activation. Bar: 20 μm; BL: baseline responses; NS: 0.9 % saline

2.4 Attenuation of Pain Hypersensitivity by Fluorocitrate into the RVM in CIBP Rats

To examine whether RVM astrocytes play a role in CIBP, fluorocitrate, a relatively selective inhibitor against astrocytes[24] was microinjected into the RVM. Either fluorocitrate (1 μg)[10] or saline was microinjected into the RVM. Mechanical allodynia was attenuated from 15 to 180 min after fluorocitrate administration, as indicated by a significant increase in PWT to 10.5±1.0 g from a pre-injection mean of 1.7±0.2 g (n=6, P<0.05) (fig. 4A). Mechanical withdrawal thresholds gradually returned to pre-injection levels (1.3±0.2 g) by 240 min, demonstrating the reversibility of fluorocitrate for behavioral responses (fig. 4A). At the time of peak effect of fluorocitrate (60–90 min after microinjection), the rats were sacrificed and RVM tissues were dissected out for immunofluorescent staining of GFAP. CIBP rats treated with saline showed a robust intensification of GFAP immunofluorescent labeling, along with the morphological changes indicative of astrocytic activation (astrocytic response score: +++) (fig. 4D). The RVM microinjection of fluorocitrate resulted in decreased GFAP immuno-labeling, indicative of reduction in activated astrocytes (astrocytic response score: +) (fig. 4E). Increased GFAP expression can be used as a measure of astrocytic activation[25]. Immuno-blotting identified a 51 kDa band that corresponded to the molecular mass of GFAP and showed a significantly increased level (84.6%±8.7%, n=3, P<0.05) in CIBP rats (fig. 4B) as compared with sham-operated animals (42.2%±8.0%; n=3). After RVM microinjection of fluorocitrate into CIBP rats, GFAP protein level showed insignificant difference from sham-operated animals receiving RVM saline injection (41.0%±6.8%, n=3, P>0.05) (fig. 4B), indicating a decrease in astrocytic activation. These results suggested that astrocytic activation was evoked in the RVM of CIBP rats and administration of fluorocitrate could profoundly diminish this activation and consequently exerted analgesia effects.

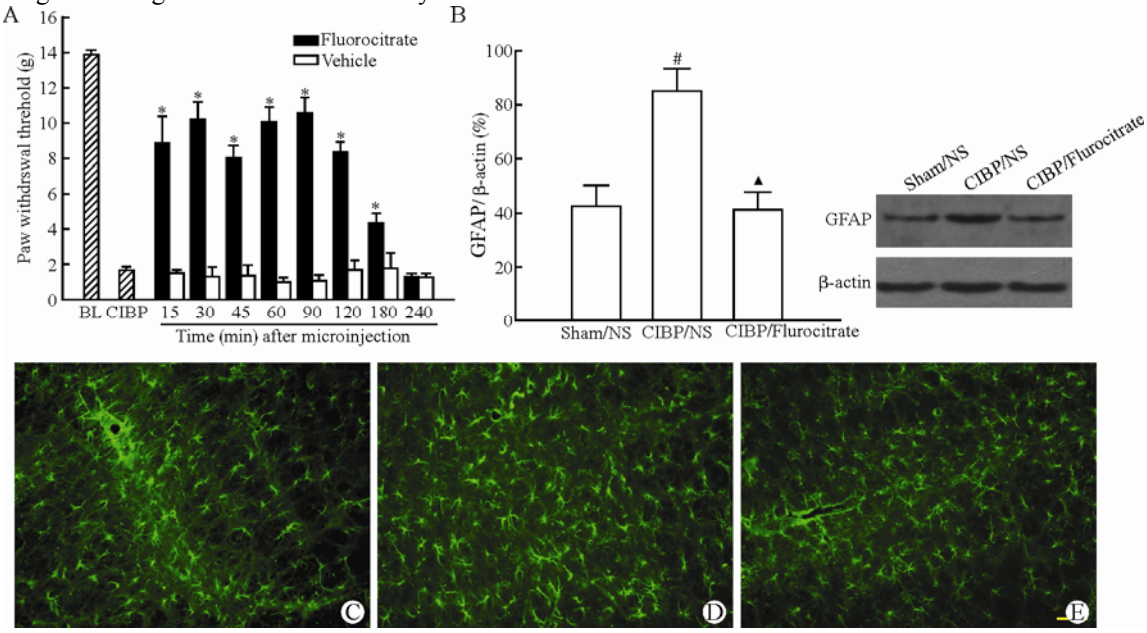

Fig. 4 Astrocytic inhibitor attenuated CIBP and reversed astrocytic activation.

A: RVM injection of fluorocitrate attenuated mechanical allodynia time-dependently ($^{*}P$<0.05, *vs.* CIBP). B: RVM injection of fluorocitrate reversed the up-regulation of GFAP in CIBP rats ($^{\#}P$<0.05, *vs.* Sham/NS; $^{\blacktriangle}P$<0.05, *vs.* CIBP/NS). C: RVM sections from sham-operated rats received saline. D: CIBP rats were given saline. E: CIBP rats were administered fluorocitrate at 1 μg.In CIBP rats, RVM injection of fluorocitrate produced a reduction in immunofluorescence intensity for GFAP along with morphological changes, suggesting reduced astrocytic activation. Bar: 20 μm; BL: baseline responses; NS: 0.9 % saline

2.5 Reversing Effect of p38 MAPK Inhibition in the RVM on Microglial Activation and Its Attenuating Action on Allodynia in CIBP Rats

Previous studies indicated that p38 MAPK phosphorylation was increased in activated microglia during both neuropathic pain[12] and inflammatory pain[10], which could promote the activated microglia to release pro-inflammatory mediators. To determine whether p38 MAPK is activated within the RVM and inhibition of p-p38 MAPK could attenuate CIBP, p38 MAPK inhibitor SB203580 (10 μg)[10] or saline was microinjected into the RVM of the animals. In CIBP rats, mechanical allodynia was attenuated 15 and 45 min after SB203580 administration, as indicated by a significant increase in PWT to 9.3±0.4 g (n=6; P<0.05) (fig. 5A). PWTs returned to pre-injection level (0.8± 0.2 g) by 90 min after administration (fig. 5A). Microinjection of saline into RVM of CIBP rats did not produce any significant changes in behavioral responses. Additional groups of CIBP rats or sham-operated rats were injected with either saline or SB203580. At the time of peak analgesic effect following SB203580 administration (30 min), the rats were sacrificed and RVM were dissected out and subsequently subjected to immunofluorescent staining for OX-42, to further determine changes in microglial activation. The tissues from CIBP rats microinjected with saline showed increased immunofluorescent intensity for OX-42 (microglial response score: +++) (fig. 5D) relative to the RVM sections from sham-operated animals receiving saline (microglial response score: 0) (fig. 5C), along with

characteristic morphological features of microglial activation (fig. 5D). On the other hand, tissues from CIBP rats treated with SB203580 showed reduced immunofluorescent intensity for OX-42, and relative resting morphological signs for microglia (microglial response score: +) (fig. 5E). In contrast, the RVM microinjection of SB203580 did not reduce immunofluorescent labeling for GFAP in CIBP rats (data not shown). Immuno-blotting identified a 43 kDa band that corresponded to the molecular weight of p-p38 MAPK and showed significantly increased level (29.5% ±1.3%, n=3; P<0.05) in CIBP rats (fig. 5B) as compared with sham-operated animals (14.5%±1.8%; n=3). After RVM microinjection of SB203580 in CIBP rats, p-p38 MAPK protein level showed an insignificant difference from that of saline-treated sham animals (12.6%±0.8%, n=3; P>0.05) (fig. 5B), indicating a decrease in p-p38 MAPK phosphorylation. These results suggested that p38 MAPK phosphorylation was induced in the RVM of CIBP rats and that administration of SB203580 abolished this activation correspondingly. Since the microglial activation was also inhibited by SB203580, the analgesic effects of SB203580 within RVM were believed to work by inhibiting local microglial p38 MAPK phosphorylation.

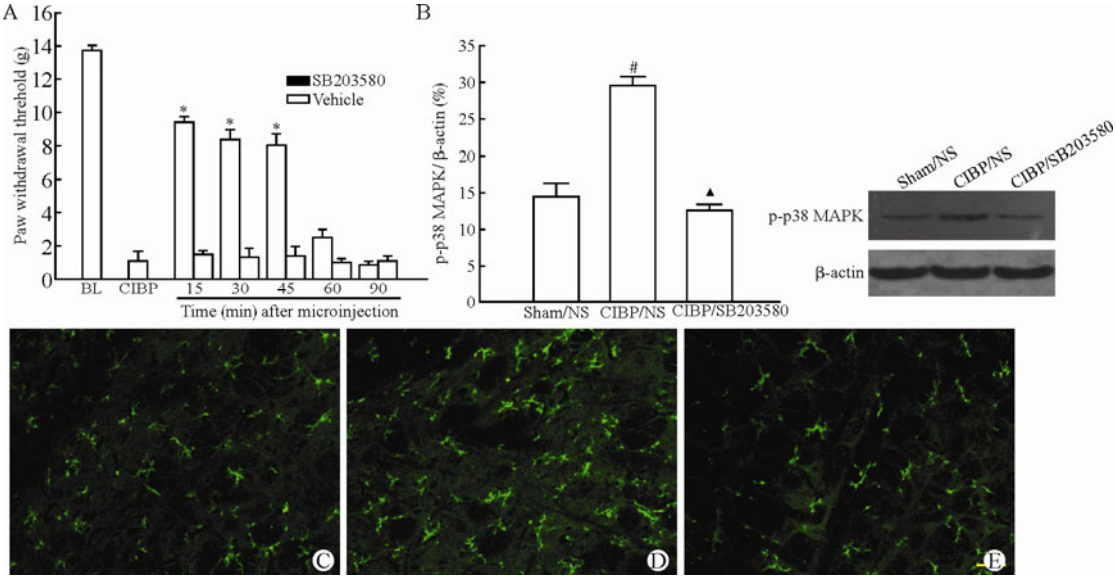

Fig. 5 Inhibition of p38 MAPK in RVM attenuated mechanical hypersensitivity in CIBP rats

A: RVM injection of p38 MAPK inhibitor SB203580 attenuated mechanical allodynia time-dependently ($^{*}P$<0.05, *vs.* CIBP). B: RVM injection of SB203580 reversed the up-regulation of p-p38 MAPK in CIBP rats ($^{\#}P$<0.05, *vs.* Sham/NS; $^{\blacktriangle}P$<0.05, *vs.* CIBP/NS). C: RVM sections from sham-operated rats receiving saline. D: RVM sections from CIBP rats given saline. E: RVM sections from CIBP rats were administered SB203580 at 10 μg. These RVM sections were labeled with OX-42 for immunofluorescent labeling of microglia. In CIBP rats, RVM injection of SB203580 produced a reduction in immunofluorescence intensity for OX-42 and relatively resting morphological signs for microglia. Bar: 20 μm.

2.6 Reversing Effect of Inhibition of p38 MAPK in the RVM on the Up-regulation of Glial Pro-inflammatory Mediators

To further study the mechanism of RVM glial activation in CIBP, the expression of glial pro-inflamatory mediators (IL-1β, IL-6, TNF-α and BDNF) in RVM was determined by using real-time quantitative PCR. RVM tissues were collected 30 min after RVM injection of SB203580 or saline. Compared with the sham/NS group, the expression of IL-1β, IL-6, TNF-α and BDNF in CIBP/NS group was significantly increased. However, RVM microinjection of p38 MAPK inhibitor reversed this up-regulation (fig. 6). Previous studies showed that the increase in p38 MAPK phosphorylation occurred mainly in activated microglia during pathologic pain. Therefore, these results suggest that the RVM microinjection of p38 MAPK inhibitor exerts its analgesic effect by inhibiting microglial p38 MAPK pathway and blocking its release of pro-inflammatory mediators.

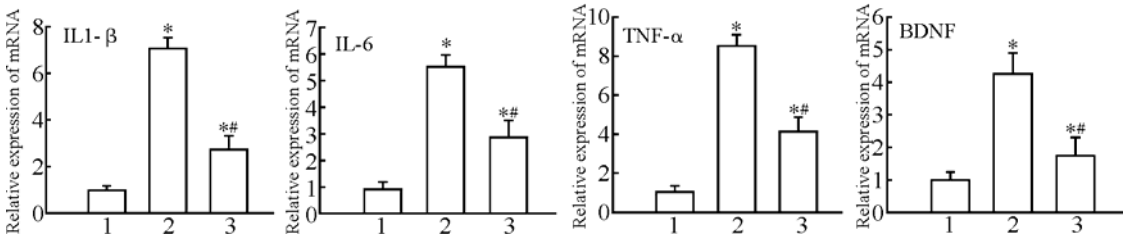

Fig. 6 RT-PCR quantification of the microglial pro-inflammatory mediators (IL-1β, IL-6, TNF-α and BDNF) in the RVM

The expression levels of IL-1β, IL-6, TNF-α and BDNF from CIBP/NS group were significantly increased (P<0.05). Thirty min after injection, RVM injection of p38 MAPK inhibitor SB203580 significantly reversed the up-regulation of IL-1β, IL-6, TNF-α and BDNF (P<0.05). $^{*}P$<0.05, *vs.* Sham/NS; $^{\#}P$<0.05, *vs.* CIBP/NS

1: Sham/NS; 2: CIBP/NS; 3: CIBP/SB203580

3 DISCUSSION

This study demonstrated microglia and astrocytes were apparently activated in the RVM of CIBP rats, and RVM microinjection of the selective microglial inhibitor or astrocytic inhibitor significantly attenuated mechanical allodynia through abolishing local activation of microglia or astrocytes, respectively. Additionally, RVM administration of p38 MAPK inhibitor relieved mechanical allodynia and reversed microglial activation and release of associated pro-inflammatory mediators in CIBP rats. Our study, for the first time, examined the roles of RVM glia in CIBP and our the findings suggest that RVM glial activation is involved in the pathogenesis of CIBP and activation of RVM microglial p38 MAPK signaling pathway contributes to descending facilitation of CIBP.

CIBP is a unique pain state with some features of neuropathy and inflammation, but it is more complicated. With CIBP, the tumor itself exerts pressure on surrounding structures, including the sensory nerves innervating the bone and periosteum. The tumor and associated immune cells release a range of pro-hyperalgesic mediators, which may sensitize peripheral nociceptors. Thus a combination of a neuropathic type nerve injury, either due to tumor compression or ischemia, and peripheral sensitization secondary to release of cytokines and other mediators, may both contribute to the chronic pain syndrome of CIBP. Moreover, factors in the bone and its microenvironment may also affect CIBP, such as hypoxia, acidic pH, and high extracellular calcium concentrations. These factors led to changes in plasticity in the central nervous system, including alterations both in neurochemistry and functional responses[1]. Because the specific mechanism of CIBP is still unclear, current pharmacological treatments are based on understanding of their mechanisms of action in non-cancer pain syndromes. Therefore, further study of the mechanism of CIBP and developing an alternative strategy to target the specific neurobiological changes of CIBP are needed.

Supra-spinal descending nociceptive facilitation system plays an important role in maintaining pathologic pain states[8], among which RVM is a particularly important relay site for integrating descending influences to the spinal cord. Recently, growing evidence suggest that, in a variety of pathologic pain states, the RVM keeps facilitating spinal sensitization, and mediates the development of pathologic pain[8]. The activated descending nociceptive facilitation could induce the release of pronociceptive excitatory neurotransmitters from primary afferent terminals and result in long-lasting sensitization of spinal neurons, which is a main cause for maintaining spinal sensitization[8]. It was previously reported that RVM microglia were activated in inflammatory pain[10] and neuropathic pain[11]. The activated glia could release cytokines such as TNF-α and IL-1β，which act on corresponding receptors on the RVM descending facilitatory neurons. Thus, supra-spinal glia and associated cytokines as well as glia-neuron interactions could contribute to the descending facilitation of pathologic pain[11]. This study demonstrated that RVM glia were activated in CIBP, and when locally treated with selective glial inhibitors, the CIBP rats showed decreased mechanical allodynia. Wei *et al* reported that in neuropathic pain RVM microglial activation occurred in the early stage, e.g., within several days after nerve injury[11]. Roberts *et al* reported that RVM microglial activation appeared within 3 hours after establishement of inflammatory model by Carrageenan[10]. In contrast, our study indicated that RVM microglial activation started at 10th day after inoculation of cancer cells, and peaked on the 15th day, then gradually decreased. This is because the CIBP model takes several days to allow cancer cells to grow in the tibial bone marrow cavity. According to our previous results and other studies, CIBP gradually increased until day 14 after inoculation when the nociceptive responses became stable [16, 26]. That means the period between day 1 and day 14 after inoculation is the early stage of CIBP. Meanwhile, the radiographic examination showed only mild bone destruction on day 10 after inoculation and severe bone destruction at the 15th day. These results suggest that RVM microglial activation occurs at the early stage of CIBP, which is consistent with what is found with neuropathic and inflammatory pain. In this study, CIBP was shown to induce RVM microglial activation and release of pro-inflammatory mediators, such as BDNF and some cytokines. Previous studies indicated that p38 MAPK phosphorylation was increased exclusively within activated microglia with both neuropathic and inflammatory pain, which promotes the activated microglia to release pro-inflammatory mediators[10, 12]. This study demonstrated that RVM injection of selective p38MAPK inhibitor inhibited microglial activation, significantly reversed the up-regulation of associated pro-inflammatory mediators and alleviated mechanical allodynia. Of interest, the time courses of action of both SB203580 and minocycline on mechanical allodynia were similar. These data suggest that the activation of RVM microglial p38 MAPK pathway contributes to the development of CIBP. Similar to microglia, activated astrocytes could also release pro-inflammatory mediators, which could act on the corresponding receptors on adjacent neurons and increase their activities[11]. Our results showed that RVM astrocytes were activated in CIBP rats and microinjection of astrocytic inhibitor fluorocitrate into RVM could attenuate CIBP in a time-dependent manner. The signals that trigger and sustain astrocyte proliferation and activation are unknown, and it is intriguing to speculate that the astroglial response occurs secondary to the microglial activation[27]. The mechanism of astrocytic activation in RVM warrants further study.

Of note, in this study, drug was given by means of rapid single RVM microinjection, which could avoid some aversive effects caused by RVM cannulation. Usually, RVM cannulation entails a longer retention time of the catheter, which tends to cause substantial injury to experimental animals, such as postoperative complications[28] and neural complications[29, 30]. Besides, as an ectogenic stimulus, RVM-implanted catheter could induce local neuroinflammation and neurodegeneration, thereby interfering with the experimental conditions. Single RVM microinjection was a minimally-invasive procedure. Compared with RVM cannulation, it could significantly exclude the manipulation-related distur-

bance and make the experimental results close to the reality to the maximum degree. The short-acting intravenous anesthetics propofol was used in this study[17], and its short action duration and lack of analgesic effect make animals wake up quickly, which makes it feasible for the researchers to reliably assay nociceptive behaviors.

In summary, the present study suggested that RVM glial activation contributed to the development of CIBP through promoting descending facilitation. Activation of microglial p38MAPK pathway is involved in the modulation of the expression of RVM pro-inflammatory mediators, which might be a part of effects of RVM microglial activation in CIBP. RVM glia might serve as a novel target for the treatment of intractable CIBP.

REFERENCES

1 Colvin L, Fallon M. Challenges in cancer pain management—bone pain. Eur J Cancer, 2008,44(8):1083-1090
2 Weilbaecher KN, Guise TA, McCauley LK. Cancer to bone: a fatal attraction. Nat Rev Cancer, 2011,11(6) 411-425
3 Jimenez-Andrade JM, Mantyh WG, Bloom AP, *et al*. Bone cancer pain. Ann N Y Acad Sci, 2010,1198: 173-181
4 Goblirsch MJ, Zwolak PP, Clohisy DR. Biology of bone cancer pain. Clin Cancer Res, 2006,12 (20):6231s-6235s
5 Millan MJ. Descending control of pain. Prog Neurobiol, 2002,66 (6):355-474
6 Vera-Portocarrero LP, Zhang ET, Ossipov MH, *et al*. Descending facilitation from the rostral ventromedial medulla maintains nerve injury-induced central sensitization. Neuroscience, 2006,140(4):1311-1320
7 Porreca F, Burgess SE, Gardell LR, *et al*. Inhibition of neuropathic pain by selective ablation of brainstem medullary cells expressing the mu-opioid receptor. J Neurosci, 2001,21(14):5281-5288
8 Ossipov MH, Dussor GO, Porreca F. Central modulation of pain. J Clin Invest, 2010,120(11):3779-3787
9 Porreca F, Ossipov MH, Gebhart GF. Chronic pain and medullary descending facilitation. Trends Neurosci, 2002, 25(6):319-325
10 Roberts J, Ossipov MH, Porreca F. Glial activation in the rostroventromedial medulla promotes descending facilitation to mediate inflammatory hypersensitivity. Eur J Neurosci, 2009,30(2):229-241
11 Wei F, Guo W, Zou S, *et al*. Supraspinal glial-neuronal interactions contribute to descending pain facilitation. J Neurosci, 2008,28(42):10 482-10 495
12 Ji RR, Suter MR. p38 MAPK, microglial signaling, and neuropathic pain. Mol Pain, 2007,3:33
13 Kohno T. Neuropathic pain and neuron-glia interactions in the spinal cord. J Anesth, 2010,24(2):325-327
14 Geis C, Graulich M, Wissmann A, *et al*. Evoked pain behavior and spinal glia activation is dependent on tumor necrosis factor receptor 1 and 2 in a mouse model of bone cancer pain. Neuroscience, 2010,169(1):463-474
15 Zhang RX, Liu B, Wang L, *et al.* Spinal glial activation in a new rat model of bone cancer pain produced by prostate cancer cell inoculation of the tibia. Pain, 2005,118(1-2): 125-136
16 Cao F, Gao F, Xu AJ, *et al*. Regulation of spinal neuroimmune responses by prolonged morphine treatment in a rat model of cancer induced bone pain. Brain Res, 2010, 1326:162-173
17 Laalou FZ, de Vasconcelos AP, Oberling P, *et al*. Involvement of the basal cholinergic forebrain in the mediation of general (propofol) anesthesia. Anesthesiology, 2008,108(5):888-896
18 Wei F, Dubner R, Zou S, *et al*. Molecular depletion of descending serotonin unmasks its novel facilitatory role in the development of persistent pain. J Neurosci, 2010,30 (25):8624-8636
19 Fox A, Medhurst S, Courade JP, *et al*. Anti-hyperalgesic activity of the cox-2 inhibitor lumiracoxib in a model of bone cancer pain in the rat. Pain, 2004,107(1-2):33-40
20 Wang Y, Li X, Cao L, *et al*. Analgesic effect of diprospan in rats with trigeminal neuralgia. J Huazhong Univ Sci Technolog [Med Sci], 2011,31(3):395-399
21 Cao F, Chen SS, Yan XF, *et al*. Evaluation of side effects through selective ablation of the mu opioid receptor expressing descending nociceptive facilitatory neurons in the rostral ventromedial medulla with dermorphin-saporin. Neurotoxicology, 2009,30(6):1096-1106
22 Wang GM, Tian XB, Chen JP, *et al*. Prevention of neuropathic pain in an animal model of spare nerve injury following oral immunization with recombinant adenovirus serotype 5-mediated NR2B gene transfer. Gene Ther, 2007,14(24):1681-1687
23 Shimizu K, Guo W, Wang H, *et al*. Differential involvement of trigeminal transition zone and laminated subnucleus caudalis in orofacial deep and cutaneous hyperalgesia: the effects of interleukin-10 and glial inhibitors. Mol Pain, 2009,5:75
24 Hosoi R, Okada M, Hatazawa J, *et al*. Effect of astrocytic energy metabolism depressant on 14C-acetate uptake in intact rat brain. J Cereb Blood Flow Metab, 2004,24(2): 188-190
25 Romero-Sandoval A, Chai N, Nutile-McMenemy N, *et al.* A comparison of spinal Iba1 and GFAP expression in rodent models of acute and chronic pain. Brain Res, 2008, 1219:116-126
26 Mao-Ying QL, Zhao J, Dong ZQ, *et al.* A rat model of bone cancer pain induced by intra-tibia inoculation of Walker 256 mammary gland carcinoma cells. Biochem Biophys Res Commun, 2006,345(4):1292-1298
27 Scholz J, Woolf CJ. The neuropathic pain triad: neurons, immune cells and glia. Nat Neurosci, 2007,10(11): 1361-1368
28 Storkson RV, Kjorsvik A, Tjolsen A, *et al*. Lumbar catheterization of the spinal subarachnoid space in the rat. J Neurosci Methods, 1996,65(2):167-172
29 Kristensen JD, Post C, Gordh T Jr, *et al*. Spinal cord morphology and antinociception after chronic intrathecal administration of excitatory amino acid antagonists in the rat. Pain, 1993,54(3):309-316
30 Tsang BK, He Z, Ma T, *et al*. Decreased paralysis and better motor coordination with microspinal versus PE10 intrathecal catheters in pain study rats. Anesth Analg, 1997,84 (3):591-594

(Received Oct. 20, 2011)